

STUDY FOR FERMION DARK MATTER PRODUCTION IN PHOTON-PHOTON COLLISION

Dao Thi Le Thuy and Le Nhu Thuc*

Faculty of Physics, Hanoi National University of Education

Abstract. Fermion dark matter (FDM) production is investigated via photon-photon collision and the cross section of the FDM production is calculated in detail. Our results are evaluated at different values of the dark matter scale Λ and the light FDM mass.

Keywords: FDM, photon, cross-section.

1. Introduction

The existence of dark matter (DM) is strongly supported by observational evidence at multiple scales through gravitational effects. The DM constitutes about 80% of the matter content of the Universe [1]. The Cosmic Microwave Background (CMB) by the PLANCK collaboration yields the following DM relic abundance [2]

$$\Omega_{DM} h^2 = 0.120 \pm 0.001 \text{ at } 90\% \text{ C.L.} \quad (1.1)$$

No one knows the nature of dark matter. It is not part of the Standard Model and seems likely that the DM is a neutral and stable weakly interacting massive particle (WIMP) on cosmological time scales. Experiments at the Large Hadron Collider (LHC) and the electron-positron linear collider (LC) will give more information about the DM as a missing energy signature [3]. In 2006, Fayet *et al.* [4] studied the influence of light DM on the core collapse supernova cooling and found that the 1 - 30 MeV mass fermion DM can explain the SN1987A energy loss rate.

Fermion and scalar two-component DM are considered [5] in which the fermion DM is assigned to a singlet fermion and scalar DM is assigned to a single scalar, both stabilized by a single Z_4 symmetry.

The fermion DM production in lepton colliders via photon-dark photon-photon exchange [6] and DM pair production inside supernova [3] had been studied in detail. In this paper, we study the process $\gamma\gamma \rightarrow \bar{\chi}\chi$ via the exchange of fermion DM, the effective interaction Lagrangian of photon (γ) and fermion DM (χ) was given by [3]

Received July 27, 2022. Revised October 17, 2022. Accepted October 24, 2022.

Contact Le Nhu Thuc, e-mail address: thucln@hnue.edu.vn

$$L_{\text{int}} = -\frac{i}{2} \bar{\chi} \sigma_{\mu\nu} (\mu_\chi + \gamma_5 d_\chi) \chi F^{\mu\nu}, \quad (1.2)$$

where $F^{\mu\nu} = \partial^\mu A^\nu - \partial^\nu A^\mu$, $\sigma_{\mu\nu} = \frac{i}{2} [\gamma^\mu, \gamma^\nu]$ is the spin tensor, $\mu_\chi = \frac{1}{\Lambda_\mu}$, $d_\chi = \frac{1}{\Lambda_d}$ respectively are the magnetic dipole moment and the electric dipole moment of the FDM.

The corresponding Feynman rule has the form

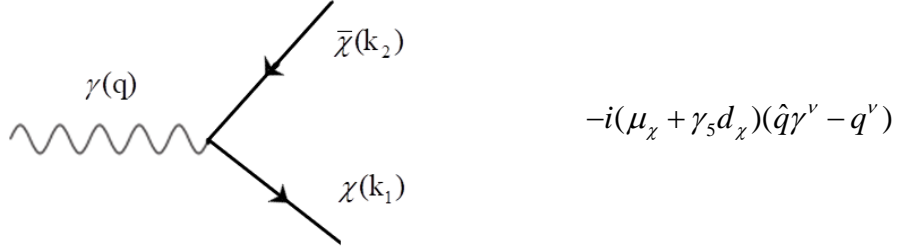


Figure 1. Feynman rule for the photon couplings with FDM

2. Content

The corresponding Feynman diagrams for the pair production of fermion DM in $\gamma\gamma$ collision via DM fermion χ exchange are shown in Figure 2.

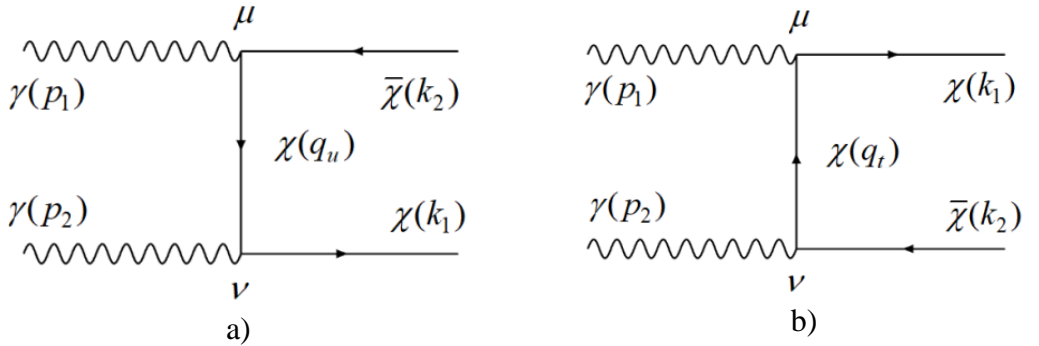


Figure 2. The Feynman diagrams for the process $\gamma\gamma \rightarrow \bar{\chi}\chi$ via DM fermion χ exchange

Applying Feynman's rule, the matrix element of the process $\gamma\gamma \rightarrow \bar{\chi}\chi$ is given by

$$M = \bar{u}(k_1, r) [-i(\mu_\chi + \gamma_5 d_\chi) (\hat{p}_2 \gamma^\nu - p_2^\nu)] \varepsilon_\nu(p_2) \frac{-i(\hat{q}_u + m_\chi)}{q_u^2 - m_\chi^2} \\ \times \varepsilon_\mu(p_1) [-i(\mu_\chi + \gamma_5 d_\chi) (\hat{p}_1 \gamma^\mu - p_1^\mu)] v(k_2, s) + \bar{u}(k_1, r) [-i(\mu_\chi + \gamma_5 d_\chi) (\hat{p}_1 \gamma^\mu - p_1^\mu)]$$

$$\times \varepsilon_\mu(p_1) \frac{-i(\hat{q}_t + m_\chi)}{q_t^2 - m_\chi^2} \varepsilon_\nu(p_2) [-i(\mu_\chi + \gamma_5 d_\chi)(\hat{p}_2 \gamma^\nu - p_2^\nu)] v(k_2, s). \quad (2.1)$$

In the center-of-mass frame, the differential cross section (DCS) for the $\gamma\gamma \rightarrow \bar{\chi}\chi$ process is given by

$$\frac{d\sigma}{d\cos\theta} = \frac{1}{32\pi s} \frac{|\vec{k}|}{|\vec{p}|} |M|^2, \quad (2.2)$$

where

$$\begin{aligned} |M|^2 = & \frac{64}{9(q_u^2 - m_\chi^2)^2} \{(\mu_\chi^2 - d_\chi^2)^2 (p_1 k_2)(p_2 k_1) [(p_1 q_u)(p_2 q_u) - (p_1 p_2) q_u^2] \\ & + m_\chi^2 [(\mu_\chi^2 + d_\chi^2)^2 + 4\mu_\chi^2 d_\chi^2] [2(p_1 p_2)(k_1 p_2) - (p_1 k_1) p_2^2]\} \\ & + \frac{64}{(q_t^2 - m_\chi^2)^2} \{2(\mu_\chi^2 - d_\chi^2)^2 (p_2 k_2)(p_1 k_1) [(p_1 q_t)(p_2 q_t) - (p_1 p_2) q_t^2] \\ & + m_\chi^2 [(\mu_\chi^2 + d_\chi^2)^2 + 4\mu_\chi^2 d_\chi^2] (p_2 k_2)(p_1 p_2)(k_1 p_1)\} \\ & + \frac{4}{(q_u^2 - m_\chi^2)(q_t^2 - m_\chi^2)} \{(\mu_\chi^2 - d_\chi^2)^2 \{-4[4(p_1 k_2)(p_2 q_u) - 2(p_1 k_2)(2(p_1 p_2) - k_2^2)] \\ & \times [(p_1 p_2)(q_t k_1) - (p_1 q_t)(p_2 k_1) + (p_1 k_1)(p_2 q_t)] \\ & - 2(p_2 p_1)(-2(p_1 k_1) + k_1^2) [2(k_2 p_1)(k_2 p_2) - k_2^2 (p_1 p_2)]\} \\ & - 16(q_u p_2)(p_1 k_1) [(k_2 p_1)(k_1 p_2) - (k_1 k_2)(p_1 p_2) + (k_2 p_2)(k_1 p_1)] \\ & - 2[8(k_2 p_2)(k_2 p_1) - 4k_2^2 (p_2 p_1)] k_1^2 (p_2 p_1) \\ & - 2[8(k_1 p_2)(p_1 k_1) - 4k_1^2 (p_1 p_2)] [(k_2 p_1)(k_2 p_2) - k_2^2 (p_1 p_2)] \\ & + 8m_\chi^2 (\mu_\chi^2 - d_\chi^2)^2 (p_1 p_2) [(p_1 k_1)(p_2 k_2) - (k_1 k_2)(p_1 p_2) + (k_2 p_1)(k_1 p_2)] \\ & - 8m_\chi^2 (\mu_\chi^2 + d_\chi^2)^2 (p_1 p_2) [(k_2 p_1)(k_1 p_2) - (k_1 k_2)(p_1 p_2) + (k_2 p_2)(k_1 p_1)] \\ & - 8m_\chi^2 (\mu_\chi^2 + d_\chi^2)(\mu_\chi^2 - d_\chi^2)(p_1 k_1) p_2^2 (p_1 k_2)\}. \end{aligned} \quad (2.3)$$

Here we used $p_1^2 = p_2^2 = m_\gamma^2 = 0$, $p_1^\mu(\sqrt{s}, \vec{p})$, $p_2^\mu(\sqrt{s}, -\vec{p})$, $k_1^\mu(\sqrt{s}, \vec{k})$, $k_2^\mu(\sqrt{s}, -\vec{k})$ and θ is the angle between \vec{p} and \vec{k} .

Next, we evaluated the dependence of the differential cross section (DCS) on the $\cos\theta$ and the center-of-mass energy \sqrt{s} in the supernova SN1987A explosion within the formalism of q-deformed statistics. In the case of the q-undeformed statistics ($q = 1$), $\Lambda_\mu = \Lambda_d = \Lambda$, when the light FDM mass increases, the bound Λ decreases. Therefore, here we choose $m_\chi = 10$ MeV corresponding to $\Lambda = 3.6 \times 10^6$ TeV and $m_\chi = 30$ MeV corresponding to $\Lambda = 3.3 \times 10^6$ TeV [3]. These results are shown in Figure 3 and Figure 4.

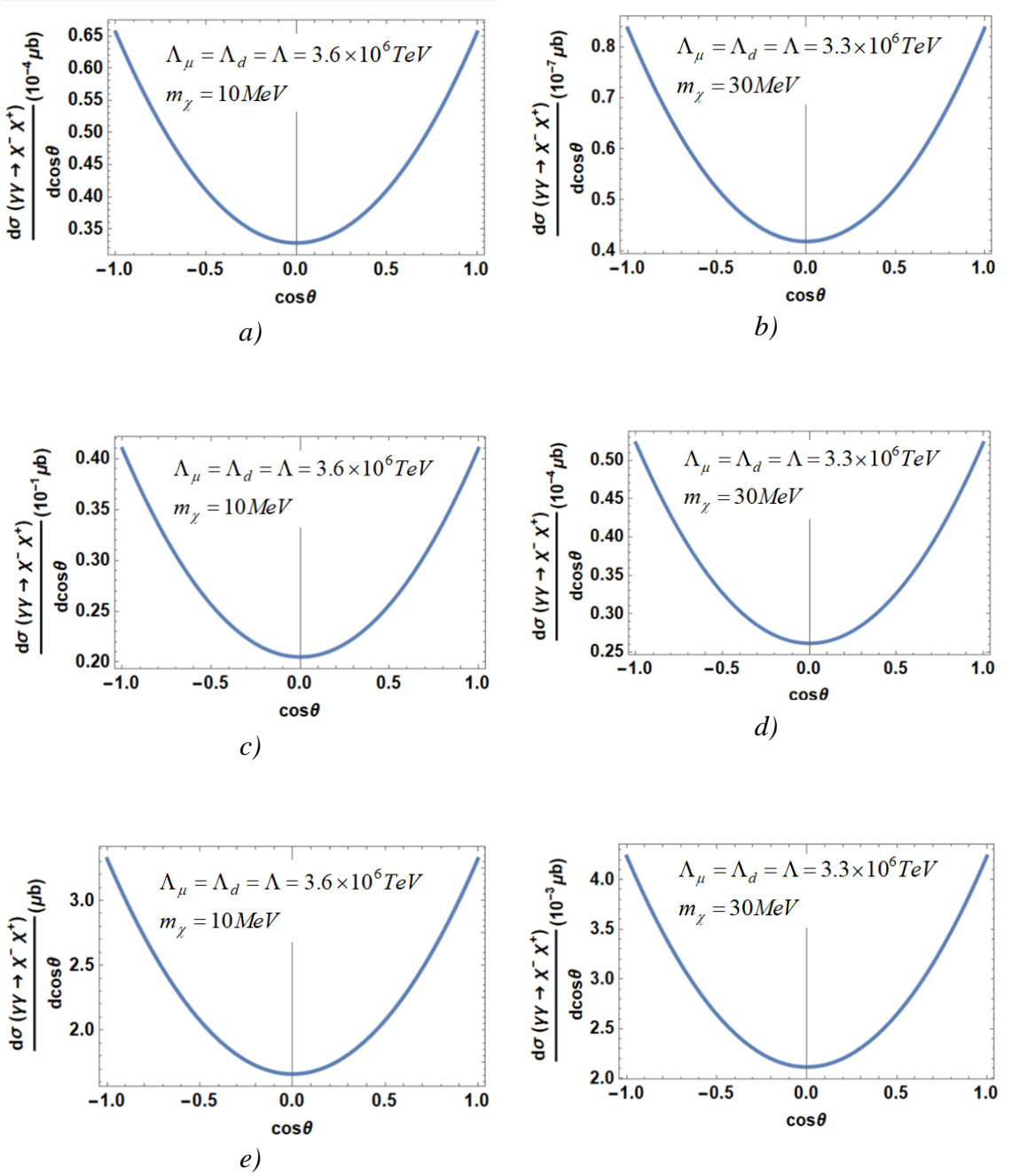


Figure 3. The DCS as a function of $\cos\theta$: (a), (b) at $\sqrt{s} = 200$ GeV; (c), (d) at $\sqrt{s} = 1000$ GeV; (e), (f) at $\sqrt{s} = 3000$ GeV

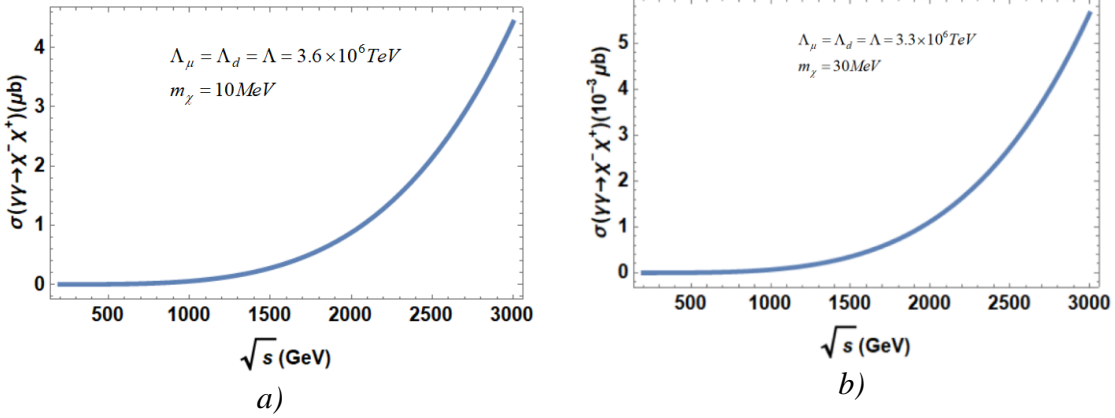


Figure 4. The total cross section as a function of \sqrt{s} : (a) at $m_\chi = 10$ MeV, (b) at $m_\chi = 30$ MeV

In Figure 3, we plotted the DCS as a function of $\cos\theta$ with $-1 \leq \cos\theta \leq 1$ at $\sqrt{s} = 200$ GeV for figures a, b; $\sqrt{s} = 1000$ GeV for figures c, d and $\sqrt{s} = 3000$ GeV for figures e, f. The results show that in all cases, the DCS gets the maximum value at $\cos\theta = \pm 1$. When $\Lambda_\mu = \Lambda_d = \Lambda = 3.6 \times 10^6$ TeV, $m_\chi = 10$ MeV, the DCS is $0.656 (10^{-4} \mu\text{b})$, $0.41 (10^{-1} \mu\text{b})$ and $3.321 (\mu\text{b})$ at $\sqrt{s} = 200$ GeV, $\sqrt{s} = 1000$ GeV and $\sqrt{s} = 3000$ GeV respectively. When $\Lambda_\mu = \Lambda_d = \Lambda = 3.3 \times 10^6$ TeV, $m_\chi = 30$ MeV, the DCS is $0.836 (10^{-7} \mu\text{b})$, $0.523 (10^{-4} \mu\text{b})$ and $0.4233 (10^{-3} \mu\text{b})$ at $\sqrt{s} = 200$ GeV, $\sqrt{s} = 1000$ GeV, $\sqrt{s} = 3000$ GeV respectively. In all cases, the DCS has the smallest value at $\cos\theta = 0$. In each case of \sqrt{s} , the maximum value of the DCS is about twice as large as the minimum value. Therefore, in the same or opposite direction for the initial photon beams, the missing energy signature is greatest. Besides, at the mass $m_\chi = 10$ MeV, the DCS is larger than at the mass $m_\chi = 30$ MeV (about 100 times). That means DM is maybe observable at low mass than at high mass. The rate of energy loss due to light FDM pair production is proportional to the total cross section [3]. In Figure 4, the cross section increases while \sqrt{s} increases. The total cross section for the mass $m_\chi = 10$ MeV increases faster and larger than that for the mass $m_\chi = 30$ MeV. This indicates that the rate of energy loss for the mass $m_\chi = 10$ MeV DM production is greater than that for the mass $m_\chi = 30$ MeV DM production.

3. Conclusions

The maximum value of the DCS is about twice as large as the minimum value. In the same or opposite direction for the initial photon beams, the missing energy signature is greatest. In addition, the cross section increases when \sqrt{s} increases and the rate of energy loss for the mass $m_\chi = 10$ MeV DM production is greater than that for the mass

$m_\chi = 30$ MeV DM production. That means DM is more observable at low mass than at high mass via the missing energy signature. The cross section is very small, however, we may be searching for light FDM from $\gamma\gamma$ collisions if interactive energy is large enough.

REFERENCES

- [1] C. Alvarado, C. Bonilla, J. Leite and J. W.F. Valle, 2021. Phenomenology of fermion dark matter as neutrino mass mediator with gauged B-L. *Phys. Lett.*, B 817, 136292.
- [2] Plank Collaboration, N. Aghanim, et al., 2018. *Plank 2018 results*. VI. Cosmological parameters, arXiv: 1807.06209 [astro-ph.CO].
- [3] Atanu. Guha, Selvaganapathy. J and Prasanta Kumar Das, 2017. Q-deformed statistics and the role of a light dark matter fermion in the supernova SN1987A cooling. *Phys. Rev.*, D 95, 015001.
- [4] P. Fayet, D. Hooper and G. Sigl, 2006. Constraints on Light Dark Matter From Core-Collapse Supernovae. *Phys. Rev. Lett.*, 96, 211302.
- [5] C. E. Yaguna and O. Zapata, 2022. Fermion and scalar two-component dark matter from a Z_4 symmetry, *Phys Rev.*, D 105, 095026.
- [6] L.N. Thuc and D.T.L. Thuy, 2019. Dark matter fermion production has been studied at lepton colliders via photon-dark photon-photon exchange. *HNUE Journal of Science*, Vol. 64, pp. 70-76.